Akademik Ziraat Dergisi 13(2): 272-286 (2024)
ISSN: 2147-6403 e-ISSN: 2618-5881 DOI: http://dx.doi.org/10.29278/azd.1522321

Araştırma
(Research)

Plackett–Burman and Box–Behnken Designs for Optimizing *Polygonum cognatum* Meissn-Mediated AgNP Synthesis: Antifungal Activity Against Diverse *Phytophthora* spp.*

Muharrem TÜRKKAN[1*], Yaren GÜREL[1]

[1]Ordu University, Faculty of Agriculture, Plant Protection Department, Ordu/TÜRKİYE

*The Scientific Research Projects Unit (BAP) of Ordu University is gratefully acknowledged for their support of this research under project number B-2217.

Alınış tarihi: 25 Temmuz 2024, Kabul tarihi: 11 Eylül 2024
Sorumlu yazar: Muharrem TÜRKKAN, e-posta: muharremturkkan@odu.edu.tr

Abstract

Objective: This study aimed to develop an eco-friendly method for synthesizing silver nanoparticles (AgNPs) using *Polygonum cognatum* (Madimak) extract and optimize their production using statistical design of experiments. The synthesized AgNPs were characterized, and their antifungal activity against *Phytophthora* species was evaluated.

Materyal ve Yöntem: Madimak extract served as a bio-reducing agent for the synthesis of AgNPs. The total and individual phenolic compound content of Madimak extract was characterized by UV–Vis spectroscopy and UHPLC analyses. Optimization of AgNP yield was conducted through Plackett–Burman and Box–Behnken designs. Characterization of synthesized AgNPs was performed using UV–Vis spectroscopy, FT–IR, SEM–EDS, and TEM. The antifungal activity of AgNPs against six *Phytophthora* species was determined through *in vitro* assays.

Results: The results of the RSM optimization revealed a high AgNP yield under the optimized conditions, with a plant material amount of 5 g, a boiling temperature of 80°C, a boiling time of 20 minutes, an $AgNO_3$ concentration of 10 mM, an extract volume of 2.5 ml, a microwave power of 600 watts, and a reaction time of 90 seconds. Characterization confirmed the formation of spherical AgNPs with an average size of 10.07 nm. FT–IR analysis indicated the role of caffeic acid in AgNP synthesis. AgNPs exhibited antifungal activity against all tested *Phytophthora* species with EC_{50}, MIC, and MFC values ranging from 47.44 to 118.80 µg ml^{-1}, 400 to 600 µg ml^{-1}, and 400 to 800 µg ml^{-1}, respectively.

Conclusion: AgNPs were successfully synthesized and the process optimized using Madimak extract in this study. The synthesized AgNPs revealed potent antifungal activity against *Phytophthora* species, indicating their potential as a sustainable alternative for managing *Phytophthora* diseases.

Keywords: *Polygonum cognatum*, green synthesis, silver nanoparticles *Phytophthora* spp., toxicity

Polygonum cognatum Meissn Aracılı AgNP Sentezini Optimize Etmek İçin Plackett–Burman ve Box–Behnken Tasarımları: Çeşitli *Phytophthora* spp.'ye Karşı Antifungal Aktivite

Öz

Amaç: Bu çalışma, *Polygonum cognatum* (Madımak) ekstraktı kullanılarak gümüş nanopartiküllerin (AgNP'ler) çevre dostu bir sentez yönteminin geliştirilmesini ve istatistiksel deney tasarımı kullanılarak üretimlerinin optimize edilmesini amaçlamıştır. Sentezlenen AgNP'ler karakterize edilmiş ve *Phytophthora* türlerine karşı antifungal aktiviteleri değerlendirilmiştir.

Materyal ve Yöntem: Madımak ekstraktı, AgNP'lerin sentezi için biyo-indirgeyici bir ajan olarak görev yapmıştır. Ekstraktın toplam ve bireysel fenolik bileşik içeriği UV–Vis spektroskopisi ve UHPLC analizleri ile karakterize edilmiştir. AgNP veriminin optimizasyonu, Plackett–Burman ve Box–Behnken tasarımları kullanılarak gerçekleştirilmiştir.

Sentezlenen AgNP'lerin karakterizasyonu UV–Vis spektroskopisi, FT–IR, SEM–EDS ve TEM kullanılarak yapılmıştır. AgNP'lerin altı *Phytophthora* türüne karşı antifungal aktivitesi *in vitro* testler yoluyla belirlenmiştir.

Araştırma Bulguları: RSM optimizasyonunun sonuçları, 5 g bitki materyali miktarı, 80°C kaynatma sıcaklığı, 20 dakikalık kaynatma süresi, 10 mM $AgNO_3$ konsantrasyonu, 2.5 ml ekstrakt hacmi, 600 watt mikrodalga gücü ve 90 saniye reaksiyon süresi ile optimize edilmiş koşullar altında yüksek AgNP verimi ortaya koymuştur. Karakterizasyon, ortalama boyutu 10.07 nm olan küresel AgNP'lerin oluşumunu doğrulamıştır. FT–IR analizi, kafeik asidin AgNP sentezindeki rolünü göstermiştir. AgNP'ler, tüm test edilen *Phytophthora* türlerine karşı EC_{50}, MIC ve MFC değerleri sırasıyla 47.44 ila 118.80 µg ml^{-1}, 400 ila 600 µg ml^{-1} ve 400 ila 800 µg ml^{-1} arasında değişen antifungal aktivite sergilemiştir.

Sonuç: Bu çalışmada, Madımak ekstraktı kullanılarak AgNP'ler başarılı bir şekilde sentezlenmiş ve süreç optimize edilmiştir. Sentezlenen AgNP'ler *Phytophthora* türlerine karşı güçlü antifungal aktivite göstererek *Phytophthora* hastalıklarının yönetiminde sürdürülebilir bir alternatif olarak potansiyellerini ortaya koymuştur.

Anahtar kelimeler: *Polygonum cognatum*, yeşil sentez, gümüş nanopartiküller, *Phytophthora* spp., toksisite

Introduction

Polygonum cognatum Meissn (Madimak), a perennial wild plant from the Polygonaceae family (Yeşilada et al., 1995), has emerged as a promising bioresource for the eco-friendly synthesis of silver (Ag) nanoparticles (NPs). In Turkish folk medicine, this edible plant is valued for its various health benefits due to diuretic, analgesic, wound-healing, and potential antidiabetic properties (Dereli et al., 2019). Nevertheless, recent scientific investigations of this material have revealed its potential for use in nanotechnology. Notably, Madimak extract is rich in biomolecules, such as phenols, flavonoids, tannins, carotenoids, and terpenoids (Bayram and Topuz, 2023; Çevik et al. 2014; Yıldırım et al. 2003), which have been demonstrated to reduce metal ions, including Ag^{+1}, Fe^{+2}, and Cu^{+2}, as well as to stabilize NPs during synthesis (Gürsoy et al. 2020; Kaplan and Tosun, 2023). This eco-friendly approach represents a sustainable alternative to traditional chemical methods. In a pioneering study, Yılmaz et al. (2021) utilized surface-enhanced Raman spectroscopy (SERS) to track chemically synthesized AgNPs and *P. cognatum*-mediated AgNPs in different maize seedling tissues.

Biological approaches utilizing plants as a renewable resource present a reliable, simple, and eco-friendly methodology for the synthesis of metallic NPs (Shah et al. 2015). Plants possess readily available biomolecules with reducing and capping properties, rendering them an especially favorable choice for nanoparticle synthesis (Ovais et al., 2018; Othman et al., 2019). A wide range of plant materials, including leaves (Martínez-Bernett et al., 2016; Le et al., 2020; Nguyen et al., 2020; Halima et al., 2021; Laime-Oviedo et al., 2023), fruits (Dhar et al., 2021; Ye et al., 2023), seeds (Maitra et al., 2023; Prakash et al., 2024), and peels (Trivedi et al., 2014; Mickky et al., 2024), have been employed to generate AgNPs. Importantly, the size and shape of these AgNPs can be precisely controlled by adjusting various process parameters, including the metalic salt concentration, reaction time, pH, temperature, and biomaterial quantity (Sharma et al., 2022). Statistical optimization methods, such as Plackett–Burman design (PBD) and response surface methodology (RSM), have been shown to significantly reduce the duration of treatment and optimize these parameters, leading to more efficient AgNP synthesis (Halima et al., 2021; Laime-Oviedo et al., 2022). While single-factor optimization offers only limited insight, PBD helps identify the most influential process parameters. RSM, often employing the Box–Behnken design (BBD), builds upon PBD to establish a mathematical model predicting the optimal conditions for AgNPs with desired characteristics. This optimized synthesis approach paves the way for developing biogenic AgNPs with potential applications in various fields (e.g., agriculture and medicine). The combination of PBD and RSM has been employed in the optimization of AgNP synthesis using ethanolic fractions (Laime-Oviedo et al., 2022) and the maximization of yield from leaf extracts of *Piper betle* and *Jatropha curcas* (Halima et al., 2021). Notably, there is a lack of literature on the application of statistical optimization techniques to maximize the yield of Madimak-AgNPs, which highlights the pioneering nature of this study.

This study aimed to maximize the yield of AgNPs synthesized using Madimak extract by employing statistical models (Plackett–Burman and Box–

Behnken designs). Subsequently, the physicochemical properties of the synthesized AgNPs were elucidated through comprehensive characterization via UV–Vis spectroscopy, FT–IR, SEM–EDS, and TEM analysis. The antifungal potential of the synthesized AgNPs was also evaluated under *in vitro* conditions.

Materials and Methods

Study materials

Polygonum cognatum specimens were collected from their natural habitat in Zara district, Sivas province, Türkiye.

All the chemicals, including silver nitrate ($AgNO_3$), sodium hydroxide (NaOH), and Agar Agar medium were purchased from Merck (Merck KGaA, Darmstadt, Germany).

Isolates of *Phytophthora* species (*P. cactorum, P. capsici, P. cinnamomi, P. citrophthora, P. nicotianae*, and *P. palmivora*) causing root and stem rots in different plants were obtained from the fungal culture collection maintained at the Department of Plant Protection, Faculty of Agriculture, Ordu University.

Preperation of aqueous Madimak extract

Freshly collected Madimak plants were washed with tap water to remove initial impurities, followed by three rinses with distilled water. To facilitate efficient extraction of bioactive compounds, the plants were then cut into smaller pieces and dried under controlled laboratory conditions. To optimize the extraction process for AgNP synthesis, we investigated the influence of various parameters: amount of plant material (5, 7.5, or 10 g), boiling time (20 or 30 min.), and temperature (60, 70, or 80°C). Accurately weighed portions of chopped Madimak were added to separate 250 ml beakers containing 100 ml of distilled water. The samples were then boiled at the predetermined temperature for the indicated time. After boiling, the extracts were cooled to room temperature, filtered through Whatman No. 1 filter paper, and centrifuged at 10,000 rpm for 10 minutes to remove any remaining plant material. Finally, the extracts were stored in a refrigerator at 4°C until use in the synthesis of AgNPs as reducing and stabilizing agents.

Analysis of Total Phenolics, Flavonoids, and Individual Phenolic Compounds in Madimak

To characterize the bioactive potential of the Madimak extract, its total phenolic and flavonoid contents were determined using a UV–Vis spectrophotometer. The methodologies proposed by Singleton and Rossi (1965) and Zhishen et al. (1999) were employed to quantify these compounds, with the results expressed as grams of gallic acid equivalents (GAE) per kilogram of fresh weight (fw) for phenolics and grams of quercetin equivalents (QE) per kilogram of fw for flavonoids (Ateş and Öztürk, 2023). Moreover, phenolic profile of the extracts was investigated using ultrahigh-performance liquid chromatography (UHPLC, Thermo Fisher Scientific Inc., Ultimate-3000, Waltham, MA, USA) with diode array detection (DAD 3000, Thermo Fisher Scientific Inc.) analysis, based on the method established by Özturk et al. (2015). This technique permitted the identification and quantification of individual phenolic compounds, including catechin, caffeic acid, chlorogenic acid, rutin, and several phenolic acids.

Synthesis of silver nanoparticles (AgNPs)

The Madimak extract, ranging from 2.5 to 5 ml, was introduced dropwise to a silver nitrate ($AgNO_3$) solution (1-10 mM). The resulting mixture (25 ml) was adjusted to a pH of 10 using a 0.1 M sodium hydroxide (NaOH) solution. Microwave irradiation (600-800 watts for 30-90 sec.) resulted in the reduction of silver ions (Ag^{+1}), causing a change in color from greenish-yellow to brown or dark brown. The formation of Madimak-stabilized AgNPs was confirmed by UV–Vis spectroscopy (200-700 nm). The yield of the synthesized nanoparticles was estimated based on the area under the spectral curve between 350 and 420 nm, which corresponds to AgNPs in the size range of 5-50 nm (Noroozi et al., 2012; Chowdhury et al., 2016). The spectral area was calculated in Microsoft Excel using the following equation (Eq. 1):

$$Y = \sum (a_i + a_{i+1})/2 \times (w_{i+1} - w_i)$$

where Y is the response (area), a is the absorbance, and w is the wavelength.

Optimization of Madimak-AgNP Synthesis

In order to maximize the yield of Madimak-AgNPs and optimize the synthesis process, two statistical design methodologies were employed: the PBD and the BBD.

Plackett–Burman Design (PBD): Unveiling Key Factors

The PBD was employed as an initial screening tool to identify the most influential factors affecting the synthesis of Madimak-AgNPs. To maximize the yield of Madimak-AgNPs, seven variables were investigated: plant material quantity (g), boiling temperature (°C), boiling time (min.), $AgNO_3$

concentration (mM), extract volume (ml), microwave power (W), and reaction time (sec.). Each of these factors was designated with a letter (A-G) and tested at two levels: high (+1) and low (-1) (Table 1). The upper and lower limits for each factor were carefully selected based on preliminary experiments to ensure a wide range of experimental conditions. A 12-run PBD matrix was generated in Microsoft Excel, encompassing all possible combinations of high and low settings for each factor. Each experiment was performed in triplicate to reduce the potential for experimental errors and to enhance the reliability of the resulting data. The spectral area (λ = 350-420 nm) of the synthesized AgNPs, as measured by UV–Vis spectroscopy, served as the response variable, providing an indirect measure of the AgNP yield. Subsequently, the spectral area data were subjected to comprehensive statistical analysis using Minitab software (version 19.2; Minitab, LLC, State College, PA, USA). PBD is based on the first order linear model equation (Eq. 2):

$$Y = \beta_0 + \sum \beta_i x_i$$

where, Y is the response (area), β_0 is the model intercept, Xi is the level of each independent variable and βi is the linear coefficient.

Regression analysis and ANOVA (analysis of variance) were employed to evaluate the significance of each factor's effect on the response variable. The statistical analysis revealed the factors that had a statistically significant impact on the yield of the Madimak-AgNPs.

Box–Behnken Design (BBD): Optimizing Key Factors

In light of the findings derived from the PBD analysis, a BBD was used to optimize the most influential factors identified in the preceding stage of the study. The focused approach aimed to optimize the synthesis conditions and achieve the highest possible yield of Madimak-AgNPs. The BBD entailed a 29-run experimental design with specific factor levels, as detailed in Table 2. Each factor was tested at three levels: low (-1), medium (0), and high (+1). This design permitted a more comprehensive investigation of the relationships between the factors and their impact on the response variable. As with the PBD, each experiment was repeated a total of three times to ensure the robustness and reliability of the results. The spectral area (λ = 350-420 nm) was again measured using UV–Vis spectroscopy and served as the response variable.

Minitab software was utilized for designing the experiments, performing regression analysis, and generating graphical representations of the data. The response variable was fitted to a second-order polynomial model, as shown in equation (Eq. 3):

$$Y = \beta_0 + \sum_i \beta_i X_i + \sum_{ii} \beta_{ii} X_i^2 + \sum_{ij} \beta_{ij} X_i X_j$$

where Y is the response, X_i is the coded level of the independent variable, β_0 is the regression coefficient, β_i is the linear coefficient, β_{ii} is the quadratic coefficient, and β_{ij} is the interaction coefficient.

The statistical analysis of the BBD data provided valuable insights into the interactions between the factors and their combined effects on the yield of the Madimak-AgNPs. The quadratic and interaction terms in the model allowed for a more nuanced understanding of the complex relationships between the factors and their influence on the synthesis process.

Characterization of Synthesized AgNPs

The AgNPs synthesized under optimal conditions were carefully examined using a variety of analytical techniques to reveal their physicochemical properties.

The presence and size of the AgNPs were confirmed using UV–Vis spectroscopy (Lambda 35, Perkin Elmer, Inc., Hopkinton, MA, USA) in the wavelength range of 200-700 nm. A diluted AgNP solution (20 µL in 2 ml of distilled water) was analyzed in a quartz cuvette after baseline correction with blank water.

Functional groups potentially associated with the AgNPs were identified using an FT–IR spectrometer (Spectrum 65, Perkin Elmer Inc.). KBr pellets containing 1 mg of AgNPs were scanned in transmittance mode across the wavenumber range of 4000-400 cm^{-1}.

The morphology and elemental composition of the AgNPs were investigated using a combined SEM (SU-1510, Hitachi High-Tech., Tokyo, Japan) and EDS system. This analysis provided valuable information about the overall shape and elemental distribution of the nanoparticles.

High-resolution images obtained using a TEM (HighTech HT7700, Hitachi High-Tech.) allowed for a closer examination of particle size and structure. ImageJ software (version 1.53i; National Institutes of Health, Bethesda, MD, USA) was used to measure the particle size based on the TEM image scale, and the size distribution was analyzed using OriginPro

software (version 9.6.5.169; OriginLab Corporation, Northampton, MA, USA).

Antifungal Efficacy of Madimak-AgNPs against *Phytophthora* Species

The antifungal efficacy of Madimak-AgNPs against *Phytophthora* species, including *P. cactorum, P. capsici, P. cinnamomi, P. citrophthora, P. nicotianae*, and *P. palmivora*, was determined using the method previously established by Gevrek et al. (2023). Madimak-AgNPs were added to sterilised V8 agar media at various concentrations (50, 100, 200, 400, 600, and 800 µg ml^{-1}), and cooled to 50°C. Aliquots of the modified medium were dispensed into Petri dishes, with unmodified V8 agar serving as the control. Mycelial discs from 7-day-old fungal cultures were placed in the center of each plate and incubated at 25°C in the dark. After fungal growth covered the control plates (4-7 days), colony diameters were measured perpendicularly to determine growth inhibition. The percentage of fungal growth inhibition (MGI) relative to that of the control was calculated using the formula: MGI (%) = [(dc - dt)/dc] × 100, where dc and dt represent the fungal growth diameters in the control and modified plates, respectively.

In order to evaluate the fungicidal efficacy of the Madimak-AgNPs, a multi-pronged approach was employed. Probit analysis using SPSS software (version 26; IBM Company, Chicago, IL, USA) was determined the concentration required for 50% fungal growth reduction (EC_{50}). In addition, the minimum inhibitory concentration (MIC), representing the lowest AgNP concentration that fully inhibits fungal growth, was determined through parallel experiments. Lastly, the minimum fungicidal concentration (MFC) was determined by transferring agar disks exhibiting no fungal growth from modified plates to fresh V8 agar plates. These disks were incubated at 25°C for 9 days. The MFC is defined as the lowest concentration of AgNPs that results in the irreversible inhibition of fungal regrowth.

Results and Discussion

Bioactive Profile of Madimak Extract and its Contribution to AgNP Synthesis

This study successfully synthesized highly efficient spherical AgNPs using a biocompatible approach with Madimak aqueous extract as the reducing and stabilizing agent. Notably, the extract exhibited significant levels of total phenolics (3.18 g kg^{-1} GAE) and flavonoids (8.16 g kg^{-1} QE). UHPLC analysis further revealed a diverse phenolic profile with caffeic acid (165.38 mg kg^{-1}) being the dominant compound. Other identified phenolics included 4-aminobenzoic acid (11.66 mg kg^{-1}), 4-hydroxybenzoic acid (5.00 mg kg^{-1}), catechin (5.09 mg kg^{-1}), chlorogenic acid (0.55 mg kg^{-1}), epicatechin (1.72 mg kg^{-1}), p-coumaric acid (11.79 mg kg^{-1}), ferulic acid (3.36 mg kg^{-1}), and rutin (1.94 mg kg^{-1}). These findings suggest that the identified phenolic compounds—in particular, caffeic acid, p-coumaric acid, and 4-aminobenzoic acid—likely play a crucial role in the bioreduction of silver ions (Ag^+) to AgNPs. This finding is consistent with previous research indicating the involvement of plant-derived phenolics in the synthesis of AgNPs. Kumar et al. (2012) attributed the reduction of Ag^+ to Ag^0 in *Terminalia chebula* extract to its polyphenol content, suggesting that these compounds have dual functions as both reducing and stabilizing agents. Similarly, Martínez-Bernett et al. (2016) reported that phenolics in mango leaf extract facilitate Ag^+ reduction to form nanoparticles. Guo et al. (2015) proposed that the structure of caffeic acid, comprising a protonated hydroxyl and carboxylic groups, enables its capacity to complex with Ag^+ ions under alkaline conditions, thus promoting reduction.

In the microwave-assisted synthesis of AgNPs, the addition of Madimak extract to an aqueous $AgNO_3$ solution resulted in a color shift from light yellow to dark brown at the completion of the reaction, indicating the formation of AgNPs through surface plasmon resonance (SPR). As illustrated in Figure 1(a), the synthesized AgNPs exhibited a distinct SPR peak at 397 nm, accompanied by the development of a dark brown color in the solution. The sharpness of the SPR peak observed in the UV–Vis spectra not only confirmed the successful reduction of Ag^+ ions but also suggested a high degree of monodispersity among the AgNPs. This observation is consistent with prior research conducted by Konwarh et al. (2011), who demonstrated a correlation between narrower SPR peaks and smaller size variations within the nanoparticle population. The position and characteristics of the SPR band are influenced by various factors beyond the size distribution. These factors include the shape, morphology, composition, and surrounding environment of the AgNPs, as reported by Kelly et al. (2003) and Stepanov (2004).

Statistical optimization of the synthesized AgNPs

Plackett–Burman Design

Table 1 presents the PBD design matrix used to identify critical parameters influencing AgNP yield, along with the corresponding yield values obtained for each set of conditions. The data indicate a significant disparity in AgNP yield (ranging from 1.66 to 38.12), highlighting the necessity for optimization to maximize production. Figure 1(b) shows the UV–Vis spectra acquired from the various experimental runs within the PBD.

Table 3 summarizes the key findings from the statistical analysis of the PBD results. The F-value and P-value indicate that the model is statistically significant and accurately describes the relationship between the investigated factors and AgNP yield. Furthermore, the high coefficient of determination (R^2=0.97) and adjusted coefficient of determination (Adj. R^2=0.93) provided substantial evidence for a robust correlation between the model predictions and the experimental data (Mickky et al., 2024).

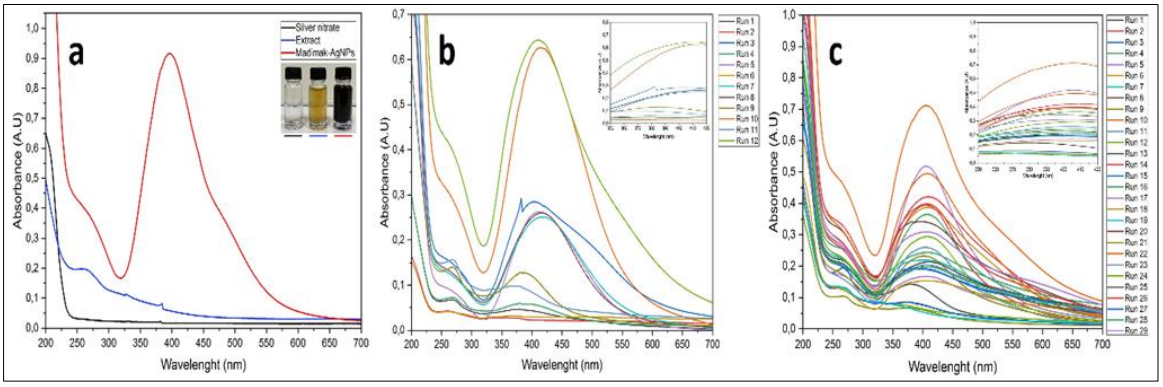

Figure 1. UV-Vis Spectra of AgNPs. (a) Synthesized under optimized conditions. (b-c) Synthesized using Plackett-Burman and Box-Behnken design parameters

Table 1. Plackett-Burman Design for Madimak-AgNP Yield: Experimental Factors, Levels, and Corresponding Yield Responses

Std	Run	Independent variables							Response Area (350-420 nm)	Predicted
		A[a]	B[b]	C[c]	D[d]	E[e]	F[f]	G[g]		
10	1	10 (+1)	60 (-1)	20 (-1)	1 (-1)	5 (+1)	600 (-1)	30 (-1)	3.08 ± 0.08	1.80
8	2	5 (-1)	80 (+1)	30 (+1)	1 (-1)	2.5 (-1)	800 (+1)	30 (-1)	1.78 ± 0.15	1.09
3	3	5 (-1)	60 (-1)	30 (+1)	10 (+1)	2.5 (-1)	600 (-1)	90 (+1)	17.61 ± 0.90	15.70
1	4	10 (+1)	60 (-1)	20 (-1)	1 (-1)	5 (+1)	600 (-1)	30 (-1)	3.92 ± 0.56	1.80
7	5	5 (-1)	80 (+1)	20 (-1)	10 (+1)	2.5 (-1)	800 (+1)	30 (-1)	14.51 ± 0.41	13.03
5	6	10 (+1)	80 (+1)	30 (+1)	10 (+1)	5 (+1)	800 (+1)	90 (+1)	40.00 ± 1.10	37.30
12	7	10 (+1)	60 (-1)	30 (+1)	10 (+1)	2.5 (-1)	600 (-1)	30 (-1)	14.32 ± 0.87	18.12
2	8	5 (-1)	80 (+1)	20 (-1)	10 (+1)	5 (+1)	600 (-1)	30 (-1)	14.81 ± 0.37	16.56
9	9	10 (+1)	60 (-1)	30 (+1)	1 (-1)	5 (+1)	800 (+1)	90 (+1)	8.05 ± 0.11	9.81
6	10	10 (+1)	80 (+1)	20 (-1)	10 (+1)	2.5 (-1)	800 (+1)	90 (+1)	35.54 ± 0.58	36.07
4	11	5 (-1)	80 (+1)	20 (-1)	1 (-1)	5 (+1)	800 (+1)	90 (+1)	6.31 ± 0.88	8.89
11	12	5 (-1)	60 (-1)	30 (+1)	1 (-1)	2.5 (-1)	600 (-1)	90 (+1)	2.15 ± 0.08	1.89

[a]Amount of plant material (g), [b]Boiling temperature (°C), [c]Boiling time (min.), [d]Concentration of $AgNO_3$ (mM), [e]Extract volume (ml), [f]Power of microwave (watt), [g]Reaction time (sec.)

Table 3. Statistical Analysis of Plackett-Burman Design for Madimak-AgNP Yield

Source	Coefficient	Effect	Contribution (%)	*F-value*	*P-value Prob > F*
Model	13.50			20.60	0.0055
A-Amount of plant material (g)	6.37	12.73	10.82	46.51	0.0109
B-Boiling temperature (°C)	6.84	13.68	33.94	18.45	0.0427
C-Boiling time (min.)	0.93	1.87	6.89	0.8118	0.5002
D-Concentration of $AgNO_3$ (mM)	6.90	13.81	32.40	79.6	0.0083
E-Extract volume (ml)	-0.32	-0.64	0.27	0.0135	0.8194
F-Power of microwave (watt)	-2.09	-4.17	0.71	2.08	0.3549
G-Reaction time (sec.)	5.15	10.31	12.28	50.64	0.0129
R^2	0.9730	Std. Dev.		3.44	
Adj. R^2	0.9258	Mean		13.5	
Pred R^2	0.7478	C.V. %		25.49	
Adeq. Precision	12.8824	PRESS		442.95	
Y = 13.50+6.37A+6.84B+0.93C+6.90D−0.32E−2.09F+5.15G (Eq. 4)					

*Significant values. "PREES: is the predicted residual sum of squares. F: Fishers's function.
P: Level of significance. C.V %: Coefficient of variation. Y: Response"

Table 3 also reveals the most influential factors affecting AgNP yield based on their *P*-values. The concentration of $AgNO_3$ emerged as the most significant factor, with a *P*-value of 0.0083, followed by the amount of plant material (*P*-value 0.0109), reaction time (*P*-value 0.0129), and boiling time (*P*-value 0.0427). A lower *P*-value indicates a greater impact of the factor on AgNP yield. The corresponding multiple linear regression model, incorporating coded values, is presented in equation 4 (see Eq. 4, Table 3).

Figure 2 illustrates the influence of individual factors on the yield of AgNPs within the PBD design. As observed in Figure 2(a) and (b), factors like plant material quantity (A), boiling temperature (B), boiling time (C), $AgNO_3$ concentration (D), and reaction time (G) exhibited a positive influence on the yield, whereas extract volume (E) and microwave power (F) appeared to have a negative effect. Statistical analysis (high *P*-values > 0.05, lower effects, and contribution percentages) suggests minimal significance for factors C, E, and F, implying they likely have a negligible impact on yield variation. Figure 2(c) presents a standardized effect plot, which visually represents the magnitude and direction of the significant factors' influence. The Pareto chart further clarifies the order of importance and absolute impact values for these factors (Figure 2d). Values exceeding the reference line are considered statistically significant, while those below are considered insignificant (Vanaja and Shobha Rani, 2007).

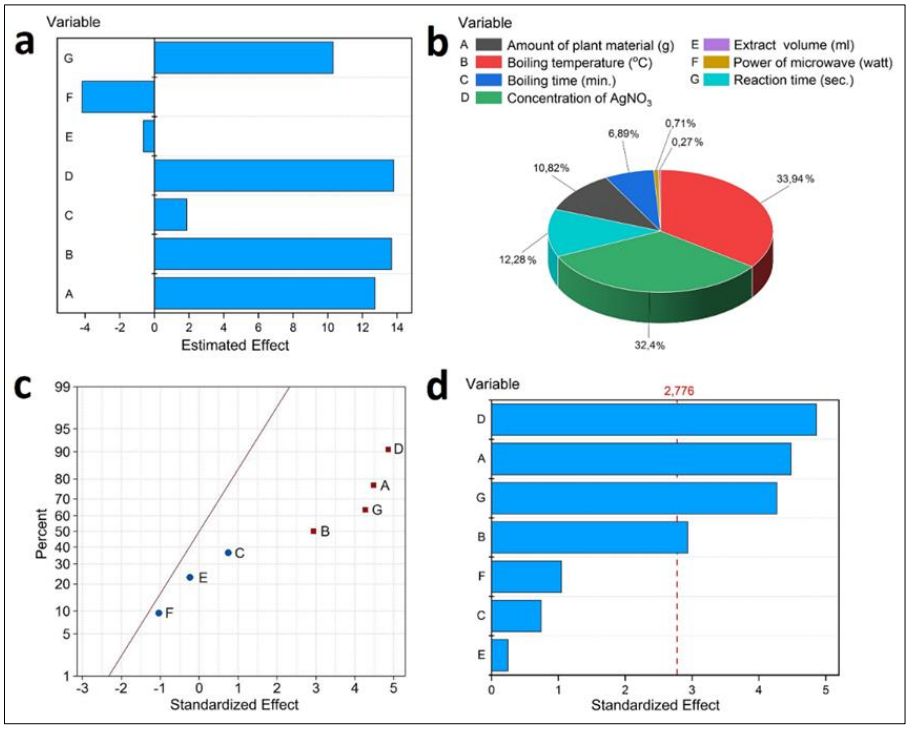

Figure 2. Identifying Key Factors for Madimak-Mediated AgNP Synthesis. (a) Estimated effects of various process variables. (b) Contribution percentage of each variable to the overall effect. (c) Normal probability plot of standardized effects to assess normality of the data. (d) Pareto chart of standardized effects to identify the most influential variables.

Based on this chart, factors A, B, D, and G emerge as the most critical parameters influencing AgNP yield. Previous research has indicated that the selection of plant species is a crucial factor in determining the critical factors for AgNP biosynthesis. In a study conducted by Trivedi et al. (2014), the authors employed PBD to investigate the influence of several factors on the synthesis of AgNPs utilizing citrus peel extract. The researchers identified temperature, illumination, and pH as the most significant parameters, while factors such as reaction volume, reductant volume, and $AgNO_3$ concentration had a lesser impact. In contrast, Halima et al. (2021) optimized AgNP biosynthesis from *Piper betle* and *Jatropha curcas* leaf extracts using PBD, identifying plant extract and $AgNO_3$ concentration as the most critical factors.

Optimization of AgNP Synthesis Parameters using Box–Behnken Design

Building upon the insights derived from the screening design, a four-factor, three-level BBD optimization approach was implemented. This strategy entailed evaluating various combinations of plant material quantities (A), boiling temperatures (B), $AgNO_3$ concentrations (D), and reaction times (G). A total of 29 experiments were conducted, and the corresponding AgNP yields, along with their UV–Vis spectra, are presented in Table 2 and Figure 1(c).

Table 2. Box-Behnken Design for Madimak-AgNP Yield: Experimental Factors, Levels, and Corresponding Yield Responses

Std*	Run	Independent variables				Response Area (350-420 nm)			Predicted
		A[a]	B[b]	D[c]	G[d]				
17	1	7.5 (0)	70 (0)	1 (-1)	90 (+1)	9.26	±	0.88	9.20
21	2	10 (+1)	70 (0)	10 (+1)	60 (0)	26.48	±	0.43	27.37
13	3	10 (+1)	60 (-1)	5.5 (0)	60 (0)	12.93	±	1.58	13.48
14	4	7.5 (0)	70 (0)	5.5 (0)	60 (0)	16.11	±	1.01	13.87
23	5	5 (-1)	70 (0)	10 (+1)	60 (0)	30.94	±	1.26	32.22
5	6	7.5 (0)	60 (-1)	10 (+1)	60 (0)	24.48	±	1.31	25.05
3	7	10 (+1)	70 (0)	5.5 (0)	30 (-1)	14.90	±	1.60	12.57
18	8	7.5 (0)	70 (0)	1 (-1)	30 (-1)	5.58	±	0.40	7.32
20	9	7.5 (0)	60 (-1)	1 (-1)	60 (0)	4.41	±	1.18	3.94
11	10	7.5 (0)	70 (0)	10 (+1)	90 (+1)	44.80	±	1.47	42.81
10	11	5 (-1)	60 (-1)	5.5 (0)	60 (0)	16.37	±	0.75	13.68
9	12	5 (-1)	70 (0)	1 (-1)	60 (0)	4.88	±	0.60	5.28
22	13	7.5 (0)	70 (0)	5.5 (0)	60 (0)	13.35	±	0.66	13.87
27	14	5 (-1)	70 (0)	5.5 (0)	90 (+1)	24.66	±	1.62	25.97
24	15	10 (+1)	70 (0)	1 (-1)	60 (0)	5.62	±	1.06	5.62
1	16	7.5 (0)	70 (0)	10 (+1)	30 (-1)	22.58	±	1.00	22.39
4	17	10 (+1)	80 (+1)	5.5 (0)	60 (0)	11.01	±	0.34	13.46
7	18	7.5 (0)	60 (-1)	5.5 (0)	30 (-1)	10.22	±	0.23	10.74
2	19	7.5 (0)	80 (+1)	1 (-1)	60 (0)	4.35	±	0.38	2.75
29	20	7.5 (0)	80 (+1)	5.5 (0)	90 (+1)	23.17	±	0.80	23.93
8	21	5 (-1)	70 (0)	5.5 (0)	30 (-1)	14.80	±	0.59	15.32
28	22	7.5 (0)	80 (+1)	10 (+1)	60 (0)	30.88	±	1.47	30.32
19	23	7.5 (0)	70 (0)	5.5 (0)	60 (0)	13.28	±	0.47	13.87
16	24	5 (-1)	80 (+1)	5.5 (0)	60 (0)	18.57	±	1.20	17.77
12	25	7.5 (0)	70 (0)	5.5 (0)	60 (0)	13.76	±	0.96	13.87
25	26	10 (+1)	70 (0)	5.5 (0)	90 (+1)	25.76	±	1.59	24.21
26	27	7.5 (0)	80 (+1)	5.5 (0)	30 (-1)	13.19	±	0.23	12.93
6	28	7.5 (0)	70 (0)	5.5 (0)	60 (0)	12.87	±	0.20	13.87
15	29	7.5 (0)	60 (-1)	5.5 (0)	90 (+1)	20.50	±	1.46	22.04

[a]Amount of plant material (g), [b]Boiling temperature (^oC), [c]Concentration of $AgNO_3$ (mM), [d]Reaction time (sec.)

Table 4 presents a summary of the principal findings resulting from the BBD statistical analysis. The results of the ANOVA of the multiple regression analysis indicate a highly significant model ($P < 0.0001$) with a strong influence, as demonstrated by the high Fisher's *F*-test value (52.03). The statistical analysis revealed that D ($AgNO_3$ concentration) and G (reaction time), along with their interaction term (DG), were statistically significant contributors to AgNP yield ($P < 0.0002$). Furthermore, the quadratic terms D^2 and G^2 also demonstrated significant effects ($P < 0.006$ and $P < 0.0001$, respectively). Conversely, the influence of factors A (plant material quantity) and B (boiling temperature) and their interaction terms (AB, AD, AG, BD, and BG) on yield was found to be nonsignificant (*P*-values > 0.1). Similarly, the quadratic terms A^2 and B^2 had no significant influence on yield. A coefficient of determination (R^2) of 0.9811 indicates a strong correlation between the model's predictions and the experimental data. The adjusted R^2 (0.9623) and predicted R^2 (0.9026) provide further evidence of the model's validity. Additional measures, including the low coefficient of variation (CV = 10.84%), mean value (16.89), adequate precision value (30.43), PRESS value (242.37), and standard deviation (1.83), collectively contributed to the model's accuracy and reliability (Table 4).

To achieve the best possible agreement between the predicted and experimental AgNP yields, a robust second-order polynomial mathematical model was developed. This model acts as a guide for optimizing the experimental design. Accordingly, the yields of the synthesized AgNPs can be estimated in terms of the independent variables by applying the following quadratic regression Eq. 5 (Table 4). For a comprehensive understanding of the interplay between factors affecting AgNP yield, 3D and 2D graphs were constructed (Figure 3 a-e). These

visualisations reveal the reciprocal effects of plant material amount, boiling temperature, $AgNO_3$ concentration and reaction time on the final yield. In general, higher yields were achieved when the boiling temperature (Figure 3a), $AgNO_3$ concentration (Figure 3b), and reaction time (Figure 3c) were maximized, while the amount of plant material was minimized (5 g). Notably, Figure 3(d) indicates that the $AgNO_3$ concentration exerts a negligible influence on the yield at a concentration of 1 mM, regardless of the boiling temperature.

Table 4. Statistical Analysis of Box-Behnken Design for Madimak-AgNP Yield

Source	df	Coefficient estimate	*F-value*	*P-value Prob > F*
Model	14	13.87	52.03	< 0.0001
A-Amount of plant material (g)	1	-1.13	4.55	0.051
B-Boiling temperature (^oC)	1	1.02	3.72	0.074
D-Concentration of $AgNO_3$ (mM)	1	12.17	530.56	< 0.0001
G-Reaction time (sec.)	1	5.57	111.24	< 0.0001
AB	1	-1.03	1.26	0.280
AD	1	-1.3	2.01	0.178
AG	1	0.2484	0.0737	0.790
BD	1	1.61	3.11	0.100
BG	1	-0.0746	0.0066	0.936
DG	1	4.63	25.64	0.0002
A^2	1	1.41	3.87	0.069
B^2	1	-0.6905	0.9229	0.353
D^2	1	2.33	10.52	0.006
G^2	1	4.23	34.56	< 0.0001
R^2	0.9811	Std. Dev.	1.83	
Adj. R^2	0.9623	Mean	16.89	
Pred R^2	0.9026	C.V. %	10.84	
Adeq. Precision	30.43	PRESS	242.37	

$Y=13.87-1.13A+1.02B+12.17D+5.57G-1.03AB-1.3AD+0.2484AG+1.61BD-0.075BG+4.64DG+1.41A^2-0.69B^2+2.33D^2+4.23G^2$ (Eq. 5)

*Significant values. "df: Degree of freedom. PREES: is the predicted residual sum of squares.
F: Fishers's function. P: Level of significance. C.V %: Coefficient of variation. Y: Response"

Similarly, Figure 3(e) indicates that the boiling temperature exerts a limited effect on the yield at a reaction time of 90 seconds. Intriguingly, Figure 3(f) highlights the synergistic interaction between the $AgNO_3$ concentration and reaction time. The highest yield was observed when both factors were at their maximum levels. These findings align with the findings of Yiğit and Türkkan (2023) and Gevrek et al. (2023), who reported similar findings for AgNPs synthesized from linden flower and hazelnut leaf extracts, respectively. In addition to our study, Cai et al. (2017) demonstrated that optimizing the "total energy" (power x time) within a specific range was crucial for synthesizing high-quality AgNPs. This finding suggested the combined influence of power and duration. Additionally, they found that insufficient total energy (<700 watts min. 100 ml^{-1}) hindered complete Ag^+ reduction, leading to poor NP formation. Similarly, Nikaeen et al. (2020) observed a parallel effect of $AgNO_3$ concentration and time on the quality of AgNPs, with higher levels of both factors leading to improved results.

Validating the Model's Predictive Power

To assess the accuracy of the Box–Behnken design model, the predicted yield of synthesized AgNPs (49.30) was compared with the actual yield obtained under the model's suggested optimal conditions. These optimal levels were: 5 g of plant material, 80°C boiling temperature, 20 min. boiling time, 10 mM $AgNO_3$ concentration, 2.5 ml extract volume, 600 watts microwave power, and 90 sec. reaction time. The experiment achieved a maximum yield of 54.66, which demonstrated a strong correlation with the model's prediction. This translates to a validation accuracy of 90.19%, confirming the model's reliability in predicting optimal AgNP synthesis conditions.

Madimak-AgNP Characterization

FT–IR spectroscopy

FT–IR analysis revealed the complex interactions of functional groups within Madimak extract, which played a pivotal role in regulating the reduction and stabilization of silver ions during the synthesis of AgNPs. Figure 4 shows a comparison of the FT–IR spectra of Madimak extract and synthesized Madimak-AgNPs in transmission mode, covering the wavenumber range of 400 cm^{-1} to 4000 cm^{-1}. FT–IR analysis revealed a broad range of peaks from 3865.35 to 3201.84 cm^{-1}, indicative of O-H stretching vibrations in hydroxyl (OH) groups potentially associated with aromatic structures and phenolic

compounds, as reported in prior studies (Jyoti et al., 2016; Kale et al., 2018; Nikaeen et al., 2020). In addition, a separate peak at 3618.46 cm^{-1} indicates the presence of C-H stretching vibrations in alkynes within the extract.

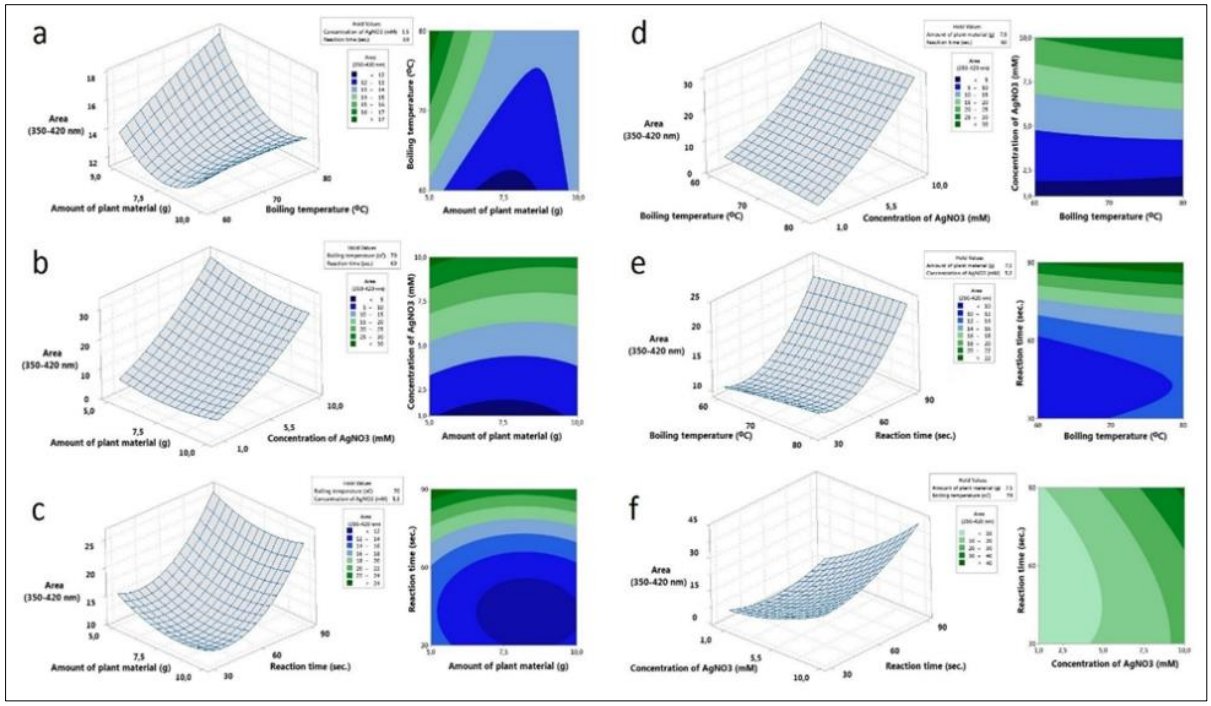

Figure 3. Impact of Process Parameters on AgNP Yield (350-420 nm): (a-c) Amount of plant material (g) vs. boiling temperature (°C), $AgNO_3$ concentration (mM), and reaction time (sec.), respectively. (d-e) Boiling temperature (°C) vs. $AgNO_3$ concentration (mM)and reaction time (sec.). (f) $AgNO_3$ concentration (mM) vs. reaction time (sec.). 3D response surfaces and corresponding 2D contour plots are presented.

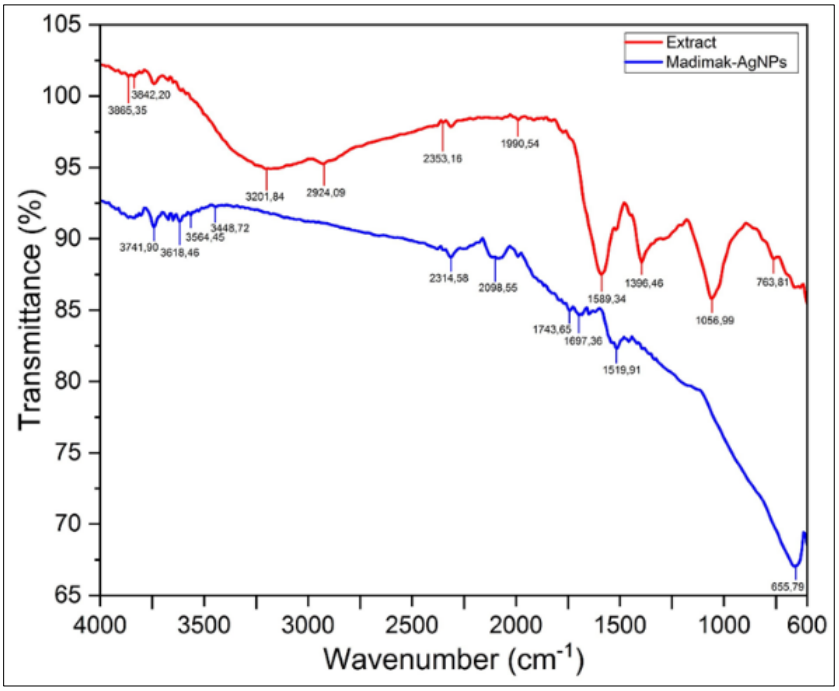

Figure 4. FT–IR Spectra of Madimak Extract and Synthesized AgNPs.

The peak at 2924.09 cm^{-1} suggested the existence of aromatic structures (C-H bonds) and potential C=C and C-OH functionalities. The spectral band at 2353.16 to 1697.36 cm^{-1} indicates the presence of various functional groups, including alkynes, carbonyls, amines, and nitriles. The FT–IR spectrum of the AgNPs exhibited a novel peak at 2098.55 cm^{-1}, within the previously observed range of 2500.00 to 1990.32 cm^{-1} (Laime-Oviedo et al., 2023), which may be attributed to reduction and stabilization. Notably, the spectrum exhibited no distinct peaks comparable to those observed in the extract (1589.34, 1396.46, 1056.99 cm^{-1}), which corresponded to C=O, C-N, and C-O stretching, respectively (Shameli et al., 2012). This absence indicates a shift in the molecular structure of these functional groups during the formation of AgNPs. The spectra exhibited the presence of common C-H stretching peaks at 763 cm^{-1} and 655.79 cm^{-1}. FT–IR analysis indicated that functional groups within the Madimak extract, particularly hydroxyl (-OH), amine (-NH), and carboxyl (-C=O) groups, play pivotal roles in facilitating the formation of AgNPs.

Microscopic and Elemental Analysis

SEM and TEM analyses (Figure 5a-c) confirmed the formation of spherical Madimak-AgNPs with good dispersion and minimal aggregation. The particle sizes ranged from 6.02 to 17.00 nm, with an average of 10.07 ± 0.16 nm (Figure 5d). Furthermore, EDS analysis (Figure 5e) revealed a distinct peak at 3 keV, confirming the presence of elemental silver (Ag) and supporting the formation of metallic Ag nanocrystals. This is further corroborated by the observed surface plasmon resonance phenomenon at 3 keV, which is characteristic of metallic Ag nanoparticles (Magudapathy et al., 2001; Vijayaraghavan et al., 2012).

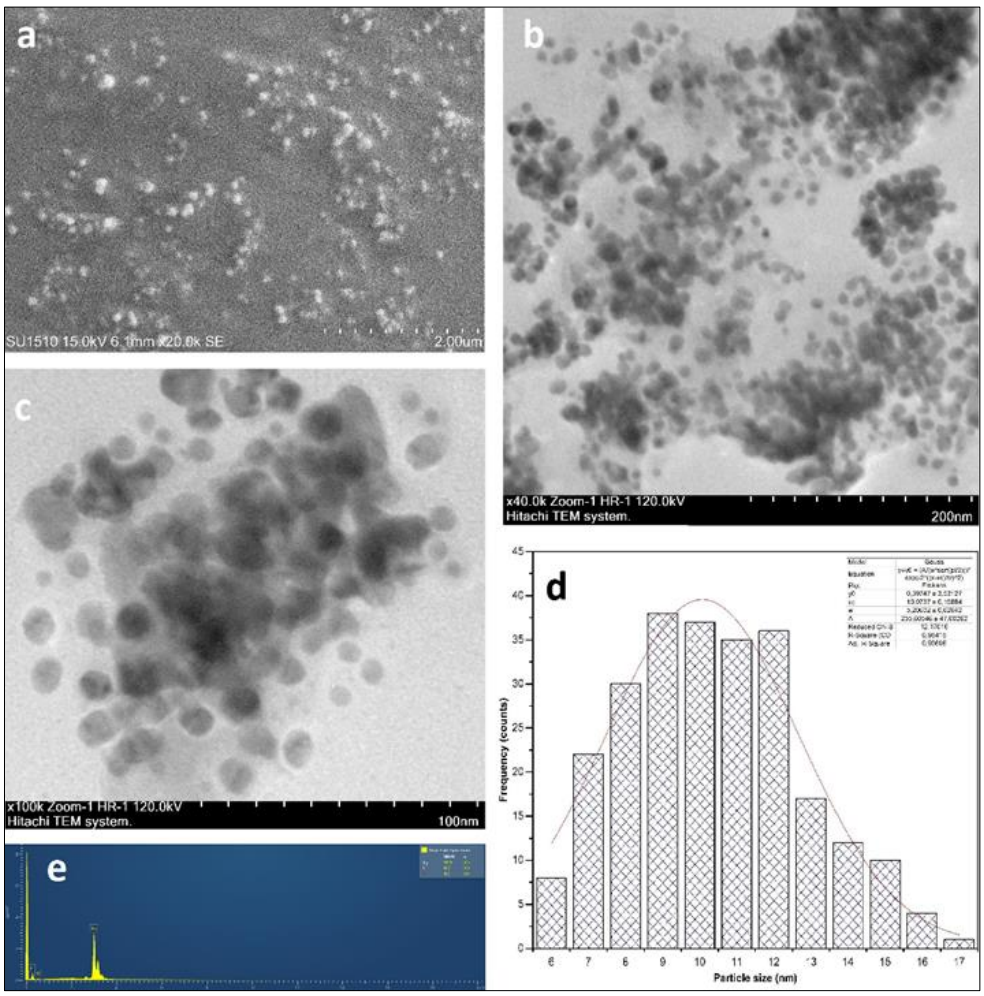

Figure 5. Characterization of Madimak-AgNPs. (a) SEM image; (b, c) TEM images at different magnifications; (d) Size distribution; (e) EDS spectrum.

Antifungal activity of the Madimak-AgNPs

The antifungal efficacy of Madimak-AgNPs was tested against six different *Phytophthora* isolates. *P. cactorum* emerged as the most susceptible fungus among the tested isolates, exhibiting the lowest EC_{50} value of only 47.44 µg ml^{-1}. The remaining isolates displayed varying degrees of susceptibility, with EC_{50} values ranging from 56.94 µg ml^{-1} for *P. cinnamomi* to 118.80 µg ml^{-1} for *P. palmivora*. Specifically, the EC_{50} values for *P. capsici*, *P. citrophthora*, and *P. nicotianae* were 84.36 µg ml^{-1}, 104.11 µg ml^{-1}, and 112.62 µg ml^{-1}, respectively. A concentration of 400 µg ml^{-1} was sufficient to completely halt the mycelial growth of *P. cactorum* when Madimak-AgNPs were used, while a higher concentration of 600 µg ml^{-1} was required for complete inhibition of the other five *Phytophthora* species. The MFC values of Madimak-AgNPs for *P. cactorum*, *P. capsici*, *P. cinnamomi*, *P. citrophthora*, *P. nicotianae*, and *P. palmivora* were 400, 600, 600, 600, 800 and 800 µg ml^{-1}, respectively (Figure 6). This aligns with the findings of Yigit and Türkkan (2023), who reported a similar MFC range (225-900 µg ml^{-1}) for linden-AgNPs against these same fungi. While several studies, such as Ali et al. (2015), reported highly effective green-synthesized AgNPs against *Phytophthora* species, others, such as Gevrek et al. (2023), observed limited antifungal activity of their green-synthesized AgNPs at the tested concentrations. The observed differences highlight the complex interplay between AgNP properties and target organisms. The toxicity of AgNPs is believed to be dependent on their size, shape, and form. Upon entering microbial cells, they disrupt essential cell organelle functions, leading to cell death (Buzea et al., 2007).

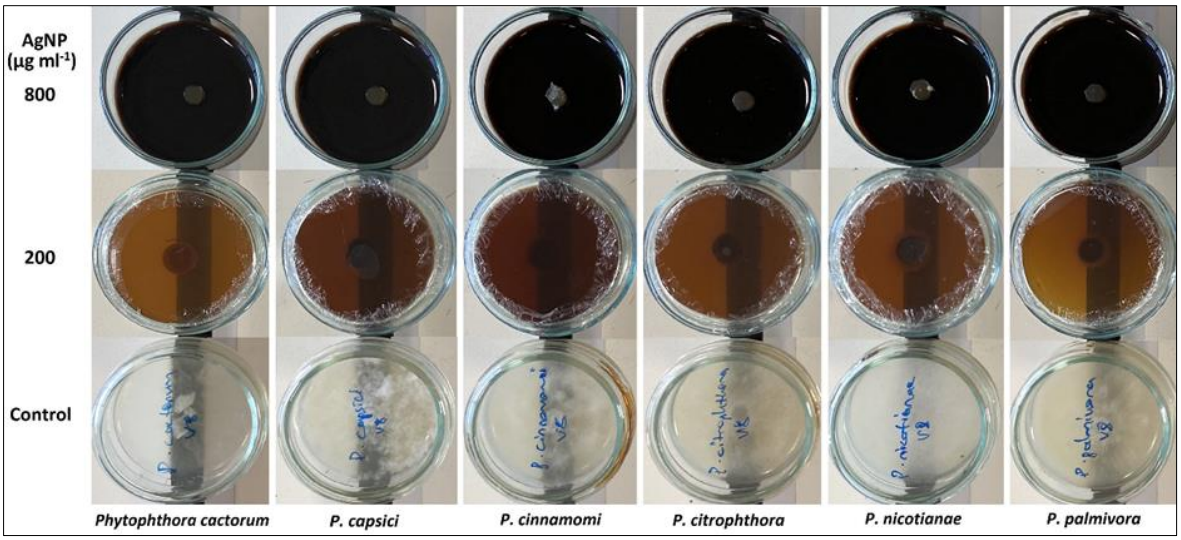

Figure 6. Inhibition of *Phytophthora* spp. Growth by Madimak-AgNPs at 200 and 800 µg ml^{-1}

Conclusion

This study investigated a green method of synthesizing AgNPs with Madimak extract. UHPLC and UV–Vis analyses revealed a rich profile of bioactive compounds in the extract, including confirmed phenolic acids and potentially flavonoids. These bioactives are likely responsible for reducing silver ions and stabilizing the resulting AgNPs. Statistical methods identified the optimal conditions for AgNP yield: 5 g of Madimak plant material, a boiling temperature of 80°C for 20 min., a 10 mM $AgNO_3$ concentration, a 2.5 ml extract volume, a 600 watt microwave power, and a 90 sec. reaction time. Characterization revealed uniform, spherical AgNPs with sizes ranging from 6.02 to 17.00 nm (average 10.07 nm). Finally, the synthesized Madimak-AgNPs exhibited notable antifungal activity against a diverse array of *Phytophthora* species, including *P. cactorum*, *P. capsici*, *P. cinnamomi*, *P. citrophthora*, *P. nicotianae*, and *P. palmivora*. These findings suggest the potential of Madimak-AgNPs as an eco-friendly alternative for controlling fungal diseases in agriculture.

Acknowledgements

This research was gratefully supported by the Scientific Research Projects Unit (BAP) of Ordu University, project number B-2217. The authors would like to express their sincere gratitude to Dr. İlker Kurbetli for providing *Phytophthora* isolates and to Dr. Umut Ateş for conducting the analysis of phenolic and flavonoid compounds in the Madimak

extract. The authors are also grateful to Dr. Mohan Kumar Kesarla for his valuable insights and critical comments, especially his suggestions on improving the FT-IR analysis, which significantly enhanced the quality of our manuscript.

Conflict of Interest

The authors declare no conflicts of interest.

Authorship Contribution Statement

M.T: Conceptualization, Methodology, Validation, Investigation, Visualization, Writing- Original draft preparation, Writing- Reviewing and Editing. Y.G: Collection of plant samples from their natural environment, preparation of extracts and synthesis of silver nanoparticles.

References

Ali, M., Kim, B., Belfield, K. D., Norman, D., Brennan, M., & Ali, G. S. (2015). Inhibition of *P.a parasitica* and *P. capsici* by silver nanoparticles synthesized using aqueous extract of *Artemisia absinthium*. *Phytopathology, 105*(9), 1183-1190.

Ates, U., & Ozturk, B. (2023). Evaluating the bioactive profile of sweet cherry (*Prunus avium* L.) cultivars: Insights into phenolic content, antioxidant activity, and individual phenolic. *Erwerbs-Obstbau, 65*(6), 2299-2304.

Bayram, M., & Topuz, S. (2023). Optimization of phenolic compound extraction using response surface method from Madimak. *Gıda, 48*(1), 118-129.

Buzea, C., Pacheco, I. I., & Robbie, K. (2007). Nanomaterials and nanoparticles: sources and toxicity. *Biointerphases, 2*(4), MR17-MR71.

Cai, Y., Piao, X., Gao, W., Zhang, Z., Nie, E., & Sun, Z. (2017). Large-scale and facile synthesis of silver nanoparticles via a microwave method for a conductive pen. *RSC Advances, 7*(54), 34041-34048.

Çevik, Ö., Şener, A., Kumral, Z. Ö., Çetinel, Ş., Altıntaş, A., Oba, R., ... & Yarat, A. (2014). Protective and therapeutic effects of *P. cognatum* aqueous extract in experimental colitis. *Marmara Pharmaceutical Journal, 18*(3), 126-134.

Chowdhury, S., Yusof, F., Faruck, M. O., & Sulaiman, N. (2016). Process optimization of silver nanoparticle synthesis using response surface methodology. *Procedia Engineering, 148*, 992-999.

Dereli, F. T. G., Ilhan, M., Kozan, E., & Akkol, E. K. (2019). Effective eradication of pinworms (*Syphacia obvelata* and *Aspiculuris tetraptera*) with *Polygonum cognatum* Meissn. *Experimental parasitology, 196*, 63-67.

Dhar, S. A., Chowdhury, R. A., Das, S., Nahian, M. K., Islam, D., & Gafur, M. A. (2021). Plant-mediated green synthesis and characterization of AgNPs using *Phyllanthus emblica* fruit extract. *Materials Today: Proceedings, 42*, 1867-1871.

Gevrek, C., Yiğit, U., & Türkkan, M. (2023). Optimization and antifungal activity of silver nanoparticles synthesized using the leaf extract of *Corylus colurna* L. (Turkish hazelnut). *Akademik Ziraat Dergisi, 12*(Özel Sayı), 159-172.

Guo, D., Dou, D., Ge, L., Huang, Z., Wang, L., & Gu, N. (2015). A caffeic acid mediated facile synthesis of silver nanoparticles with powerful anti-cancer activity. *Colloids and Surfaces B: Biointerfaces, 134*, 229-234.

Gürsoy, N., Elagöz, S., & Gölge, E. (2020). Investigation of antimicrobial effects of silver nanoparticles (AgNPs) synthesized on *Polygonum cognatum* Meissn. and fungus environment. *Türk Tarım ve Doğa Bilimleri Dergisi, 7*(1), 221-230.

Halima, R., Narula, A., & Sravanthi, V. (2021). Optimization of process parameters for the green synthesis of silver nanoparticles using Plackett–Burman and 3-level Box–Behnken Design. *Journal of Huazhong University of Science and Technology* ISSN, 1671, 4512.

Jyoti, K., Baunthiyal, M., & Singh, A. (2016). Characterization of silver nanoparticles synthesized using *Urtica dioica* Linn. leaves and their synergistic effects with antibiotics. *Journal of Radiation Research and Applied Sciences, 9*(3), 217-227.

Kale, R., Barwar, S., Kane, P., & More, S. (2018). Green synthesis of silver nanoparticles using papaya seed and its characterization. *International Journal for Research in Applied Science & Engineering Technology, 6*, 168-174.

Kaplan, Ö., & Tosun, N. G. (2023). Biosynthesis of iron, copper and silver nanoparticles using *Polygonum cognatum* and *Tragopogon porrifolius* extracts and evaluation of their antimicrobial potentials. *Düzce Üniversitesi Bilim ve Teknoloji Dergisi, 11*(4), 2155-2167.

Kelly, K. L., Coronado, E., Zhao, L. L., & Schatz, G. C. (2003). The optical properties of metal nanoparticles: the influence of size, shape, and dielectric environment. *The Journal of Physical Chemistry B, 107*(3), 668-677.

Khan, M., Khan, A. U., Alam, M. J., Park, S., & Alam, M. (2020). Biosynthesis of silver nanoparticles and its application against phytopathogenic bacterium and fungus. *International Journal of Environmental Analytical Chemistry, 100*(12), 1390-1401.

Konwarh, R., Karak, N., Sawian, C. E., Baruah, S., & Mandal, M. (2011). Effect of sonication and aging on the templating attribute of starch for "green" silver nanoparticles and their interactions at bio-interface. *Carbohydrate Polymers, 83*(3), 1245-1252.

Kumar, K. M., Sinha, M., Mandal, B. K., Ghosh, A. R., Kumar, K. S., & Reddy, P. S. (2012). Green synthesis of silver nanoparticles using *Terminalia chebula* extract at room temperature and their antimicrobial studies. *Spectrochimica Acta Part A: Molecular and Biomolecular Spectroscopy, 91*, 228-233.

Laime-Oviedo, L. A., Soncco-Ccahui, A. A., Peralta-Alarcon, G., Arenas-Chávez, C. A., Pineda-Tapia, J. L., Díaz-Rosado, J. C., ... & Vera-Gonzales, C. (2022). Optimization of synthesis of silver nanoparticles conjugated with *Lepechinia meyenii* (Salvia) using Plackett–Burman Design and Response Surface Methodology—preliminary antibacterial activity. *Processes, 10*(9), 1727.

Laime-Oviedo, L. A., Arenas-Chávez, C. A., Yáñez, J. A., & Vera-Gonzáles, C. A. (2023). Plackett–Burman design in the biosynthesis of silver nanoparticles with *Mutisia acuminatta* (Chinchircoma) and preliminary evaluation of its antibacterial activity. *F1000Research*, 12.

Le, N. T. T., Nguyen, D. H., Nguyen, N. H., Ching, Y. C., Pham Nguyen, D. Y., Ngo, C. Q., ... & Hoang Thi, T. T. (2020). Silver nanoparticles ecofriendly synthesized by *Achyranthes aspera* and *Scoparia dulcis* leaf broth as an effective fungicide. *Applied Sciences, 10*(7), 2505.

Magudapathy, P., Gangopadhyay, P., Panigrahi, B. K., Nair, K. G. M., & Dhara, S. (2001). Electrical transport studies of Ag nanoclusters embedded in glass matrix. *Physica B: Condensed Matter, 299*(1-2), 142-146.

Maitra, B., Khatun, M. H., Ahmed, F., Ahmed, N., Kadri, H. J., Rasel, M. Z. U., ..& Rabbi, M. A. (2023). Biosynthesis of *Bixa orellana* seed extract mediated silver nanoparticles with moderate antioxidant, antibacterial and antiproliferative activity. *Arabian Journal of Chemistry, 16*(5), 104675.

Martínez-Bernett, D., Silva-Granados, A., Correa-Torres, S. N., & Herrera, A. (2016). Chromatographic analysis of phytochemicals components present in *Mangifera indica* leaves for the synthesis of silver nanoparticles by $AgNO_3$ reduction. In Journal of Physics: Conference Series (Vol. 687, No. 1, p. 012033). IOP Publishing.

Mickky, B., Elsaka, H., Abbas, M., Gebreil, A., & Eldeen, R. S. (2024). Plackett–Burman screening of physico-chemical variables affecting Citrus peel-mediated synthesis of silver nanoparticles and their antimicrobial activity. *Scientific Reports, 14*(1), 8079.

Nguyen, D. H., Lee, J. S., Park, K. D., Ching, Y. C., Nguyen, X. T., Phan, V. G., & Hoang Thi, T. T. (2020). Green silver nanoparticles formed by *Phyllanthus urinaria*, *Pouzolzia zeylanica*, and *Scoparia dulcis* leaf extracts and the antifungal activity. *Nanomaterials, 10*(3), 542.

Nikaeen, G., Yousefinejad, S., Rahmdel, S., Samari, F., & Mahdavinia, S. (2020). Central composite design for optimizing the biosynthesis of silver nanoparticles using *Plantago major* extract and investigating antibacterial, antifungal and antioxidant activity. *Scientific Reports, 10*(1), 9642.

Noroozi, M., Zakaria, A., Moksin, M. M., Wahab, Z. A., & Abedini, A. (2012). Green formation of spherical and dendritic silver nanostructures under microwave irradiation without reducing agent. *International Journal of Molecular Sciences, 13*(7), 8086-8096.

Ovais, M., Khalil, A. T., Islam, N. U., Ahmad, I., Ayaz, M., Saravanan, M., ... & Mukherjee, S. (2018). Role of plant phytochemicals and microbial enzymes in biosynthesis of metallic nanoparticles. *Applied Microbiology and Biotechnology, 102*, 6799-6814.

Othman, L., Sleiman, A., & Abdel-Massih, R. M. (2019). Antimicrobial activity of polyphenols and alkaloids in Middle eastern plants. *Front. Microbiology 10,* 911.

Özturk, B., Yıldız, K., & Küçüker, E. (2015). Effect of pre-harvest methyl jasmonate treatments on ethylene production, water-soluble phenolic compounds and fruit quality of Japanese plums. *Journal of the Science of Food and Agriculture, 95*(3), 583-591.

Prakash, S. H., Rajeshkumar, S., Khan, M. A., Prabu, C. S., Khan, M. R., Arunkumar, E., & Mohana Roopan, S. (2024). Enhancing fruit preservation: Fungal growth inhibition with grape seed-mediated Ag@AgCl nanoparticles through desirability-based optimization. *ChemistrySelect, 9*(12), e202304485.

Shah, M., Fawcett, D., Sharma, S., Tripathy, S. K., & Poinern, G. E. J. (2015). Green synthesis of metallic

nanoparticles via biological entities. Materials, 8(11), 7278-7308.

Shameli, K., Bin Ahmad, M., Jaffar Al-Mulla, E. A., Ibrahim, N. A., Shabanzadeh, P., Rustaiyan, A., ... & Zidan, M. (2012). Green biosynthesis of silver nanoparticles using *Callicarpa maingayi* stem bark extraction. *Molecules, 17*(7), 8506-8517.

Sharma, N. K., Vishwakarma, J., Rai, S., Alomar, T. S., AlMasoud, N., & Bhattarai, A. (2022). Green route synthesis and characterization techniques of silver nanoparticles and their biological adeptness. *ACS Omega, 7*(31), 27004-27020.

Singleton, V. L., & Rossi, J. A. (1965). Colorimetry of total phenolics with phosphomolybdic-phosphotungstic acid reagents. *American journal of Enology and Viticulture, 16*(3), 144-158.

Stepanov, A. L. (2004). Optical properties of metal nanoparticles synthesized in a polymer by ion implantation: a review. *Technical Physics, 49*, 143-153.

Trivedi, P., Khandelwal, M., & Srivastava, P. (2014). Statistically optimized synthesis of silver nanocubes from peel extracts of *Citrus limetta* and potential application in waste water treatment. *Journal of Mic. & Biochemical Technology, 4*(004).

Vanaja, K., & Shobha Rani, R. H. (2007). Design of experiments: concept and applications of Plackett Burman design. *Clinical Research and Regulatory Affairs, 24*(1), 1-23.

Vijayaraghavan, K., Nalini, S. K., Prakash, N. U., & Madhankumar, D. J. M. L. (2012). Biomimetic synthesis of silver nanoparticles by aqueous extract of *Syzygium aromaticum*. *Materials Letters*, *75*, 33-35.

Ye, M., Yang, W., Zhang, M., Huang, H., Huang, A., & Qiu, B. (2023). Biosynthesis, characterization, and antifungal activity of plant-mediated silver nanoparticles using *Cnidium monnieri* fruit extract. *Frontiers in Microbiology*, *14*, 1291030.

Yeşilada, E., Honda, G., Sezik, E., Tabata, M., Fujita, T., Tanaka, T., ... & Takaishi, Y. (1995). Traditional medicine in Turkey. V. Folk medicine in the inner Taurus Mountains. *Journal of Ethnopharmacology, 46*(3), 133-152.

Yılmaz, M., Yılmaz, A., Karaman, A., Aysin, F., & Aksakal, O. (2021). Monitoring chemically and green-synthesized silver nanoparticles in maize seedlings via surface-enhanced Raman spectroscopy (SERS) and their phytotoxicity evaluation. *Talanta*, *225*, 121952.

Yıldırım, A., Mavi, A., & Kara, A. A. (2003). Antioxidant and antimicrobial activities of *Polygonum cognatum* Meissn extracts. *Journal of the Science of Food and Agriculture, 83*(1), 64-69.

Yiğit, U., & Türkkan, M. (2023). Antifungal activity and optimization procedure of microwave-synthesized silver nanoparticles using linden (*Tilia rubra* subsp. *caucasica*) flower extract. *International Journal of Chemistry and Technology*, *7*(1), 25-37.

Zhishen, J., Mengcheng, T., & Jianming, W. (1999). The determination of flavonoid contents in mulberry and their scavenging effects on superoxide radicals. *Food Chemistry*, *64*(4), 555-559.